



UvA-DARE (Digital Academic Repository)

Structure and magnetic properties of $\text{SmMn}_2(\text{Ge}_{1-x}\text{Si}_x)_2$

Wang, Y.G.; Yang, F.M.; Tang, N.; Hu, J.F.; Zhu, K.W.; Chen, C.P.; Wang, Q.D.; de Boer, F.R.

DOI

[10.1063/1.363760](https://doi.org/10.1063/1.363760)

Publication date

1996

Published in

Journal of Applied Physics

[Link to publication](#)

Citation for published version (APA):

Wang, Y. G., Yang, F. M., Tang, N., Hu, J. F., Zhu, K. W., Chen, C. P., Wang, Q. D., & de Boer, F. R. (1996). Structure and magnetic properties of $\text{SmMn}_2(\text{Ge}_{1-x}\text{Si}_x)_2$. *Journal of Applied Physics*, 80, 6898-6902. <https://doi.org/10.1063/1.363760>

General rights

It is not permitted to download or to forward/distribute the text or part of it without the consent of the author(s) and/or copyright holder(s), other than for strictly personal, individual use, unless the work is under an open content license (like Creative Commons).

Disclaimer/Complaints regulations

If you believe that digital publication of certain material infringes any of your rights or (privacy) interests, please let the Library know, stating your reasons. In case of a legitimate complaint, the Library will make the material inaccessible and/or remove it from the website. Please Ask the Library: <https://uba.uva.nl/en/contact>, or a letter to: Library of the University of Amsterdam, Secretariat, Singel 425, 1012 WP Amsterdam, The Netherlands. You will be contacted as soon as possible.

Structure and magnetic properties of $\text{SmMn}_2(\text{Ge}_{1-x}\text{Si}_x)_2$

Yin-gang Wang, Fuming Yang, N. Tang, Jifan Hu, and Kaiwen Zhou

State Key Laboratory of Magnetism, Institute of Physics, Chinese Academy of Sciences, P.O. Box 603, Beijing 100080, People's Republic of China

Changpin Chen and Qidong Wang

Department of Materials Science and Engineering, Zhejiang University, Hangzhou, 310027, People's Republic of China

F. R. de Boer

Van der Waals-Zeeman Institute, University of Amsterdam, Valckenierstraat 65, 1018 XE, Amsterdam, The Netherlands

(Received 21 December 1995; accepted for publication 26 August 1996)

The structure and magnetic properties of $\text{SmMn}_2(\text{Ge}_{1-x}\text{Si}_x)_2$ compounds ($x=0-1.0$) have been investigated. All the compounds crystallize in ThCr_2Si_2 -type structure. Substitution of Si for Ge leads to a linear decrease of the lattice constants and the unit-cell volume. In all compounds a transition from the ferromagnetic to the antiferromagnetic state is observed at a lower temperature T_1 , which first decreases, goes through a minimum at $x=0.4-0.6$, and then increases again with Si concentration. As temperature increases, for the compounds with $x<0.3$ both an antiferromagnetic-ferromagnetic transition and the ferromagnetic-paramagnetic transitions are observed as well at T_2 and at the Curie temperature T_c , respectively. With increasing Si content the T_c decreases, whereas T_2 increases from 140 K for $x=0$ to 215 K for $x=0.2$. For compounds with $x\geq 0.3$ the antiferromagnetic-paramagnetic transition was observed with increasing temperature and the Néel temperature increases with increasing Si content. The saturation magnetization at 1.5 K decreases first, goes through a minimum at $x=0.6$, and then increases again with increasing Si content. At room temperature, the saturation magnetization decreases monotonically from $3.27 \mu_B/\text{f.u.}$ for $x=0$ to nearly zero for $x=0.3$. © 1996 American Institute of Physics. [S0021-8979(96)02423-1]

INTRODUCTION

The ternary RMn_2X_2 compounds (R is rare earth, X is Ge or Si) crystallize in the body-centered-tetragonal ThCr_2Si_2 type of structure with space group $I4/mmm$, in which the R, Mn, and X atoms occupy the $2a$, $4d$, and $4c$ sites, respectively.^{1,2} This structure can be described as a stacking of atomic layers with the sequence -Mn-X-R-X-Mn- along the c axis. The magnetic properties of RMn_2X_2 have been investigated by several groups.³⁻⁷ It has been established that at room temperature SmMn_2Ge_2 is a ferromagnet with Curie temperature 350 K, whereas SmMn_2Si_2 is an antiferromagnet with Néel temperature 398 K.⁷ The magnetic properties of RMn_2X_2 compounds are very sensitive to the Mn-Mn distance, particularly to the intralayer Mn-Mn distance $R_{\text{Mn-Mn}}^a$. There is a critical value of $R_{\text{Mn-Mn}}^a$, about 2.85 Å, below which the coupling between the Mn moments within the layer is antiferromagnetic and above which this coupling is ferromagnetic.^{3,4} With changing temperature, the RMn_2X_2 compounds exhibit very interesting magnetic behavior.^{2,5} In SmMn_2Ge_2 , three different magnetic ordering types have been observed: ferromagnetism for $153 \text{ K} < T < 341 \text{ K}$ (Curie temperature), antiferromagnetism for $106.5 \text{ K} < T < 153 \text{ K}$, and reentrant ferromagnetism below 106.5 K.⁶ Brabers *et al.*^{5,8} have found a field-induced magnetoresistance effect in the SmMn_2Ge_2 compound, associated with the transition from the antiferromagnetic to the ferromagnetic state. This magnetoresistance effect appearing in a bulk material may be more heartening for practical application.

A suitable element substitution is usually used not only for improving the performances of the magnetic materials,

but also for examine the mechanism of the physical properties. The present article deals with the influence of substitution of Si for Ge on the crystal structure and on magnetic properties of $\text{SmMn}_2(\text{Ge}_{1-x}\text{Si}_x)_2$ compounds.

EXPERIMENT

The $\text{SmMn}_2(\text{Ge}_{1-x}\text{Si}_x)_2$ compounds with $x=0, 0.1, 0.2, 0.3, 0.4, 0.6, 0.8, 0.9,$ and 1.0 were prepared by arc melting under argon atmosphere. For ensuring homogeneity, the sample ingots were turned over and remelted several times, followed by annealing at 1073 K for 2 weeks in an evacuated quartz tube. Purity of the metals used in the sample preparation was 99.9% for Sm and Mn, and 99.999% for Ge and Si, respectively. X-ray powder diffraction with $\text{Cu } K\alpha$ radiation was used to check the crystal structure and determine lattice parameters. The thermal magnetic behavior of the samples was measured in an applied magnetic field of 0.04 T and in the temperature range 1.5–300 K in an extracting sample magnetometer (ESM) and above 300 K in a vibrating sample magnetometer (VSM). The magnetic transition temperatures were derived from the thermal magnetic curves by extrapolating M^2 vs T plots to $M^2=0$. The magnetic susceptibility was studied in the temperature range from 300 to 1000 K in a magnetic field of 1.2 T by means of a Faraday balance. The Néel temperature is defined by the cusp maximum of $\chi(T)$, corresponding to the zero crossing of $d\chi/dT$. The magnetization as a function of the external magnetic field was measured on the samples consisting of powder particles, which were free to orient themselves in the applied magnetic field,

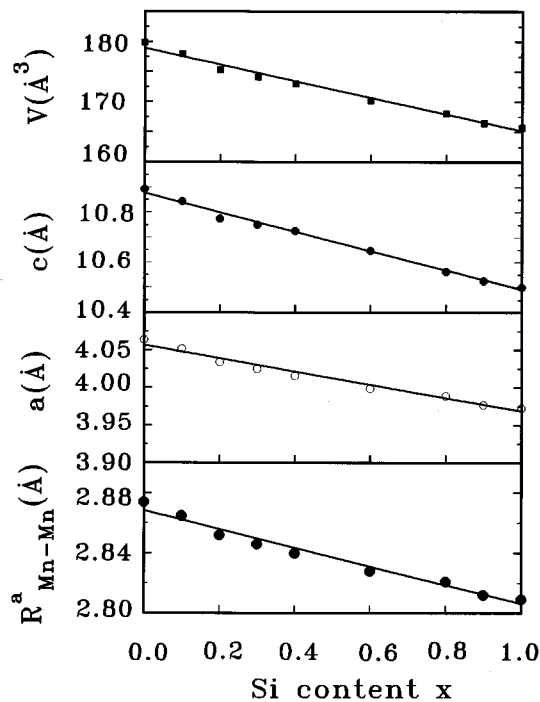


FIG. 1. The lattice constants a and c , the unit-cell volume V , and the intralayer nearest Mn–Mn distance $R_{\text{Mn–Mn}}^a$ as a function of Si concentration x for the $\text{SmMn}_2(\text{Ge}_{1-x}\text{Si}_x)_2$ compounds.

at 1.5 K in an ESM with a superconducting magnet up to 7 T and at room temperature in pulsed magnetic fields up to 10 T. The saturation magnetization was derived by extrapolating the high-field parts of M vs $1/B$ plots to $1/B=0$.

RESULTS AND DISCUSSION

The crystal structures of the $\text{SmMn}_2(\text{Ge}_{1-x}\text{Si}_x)_2$ compounds were analyzed by x-ray powder diffraction using $\text{Cu } K\alpha$ radiation. It was found that all compounds investigated are single phase and crystallize in ThCr_2Si_2 -type structure. The lattice constants a and c , derived from the x-ray-diffraction patterns by using a least-squares program, and the unit-cell volume V are presented as function of Si concentration x in Fig. 1 and the values are listed in Table I. It can be seen that substitution of Si for Ge results in a linear decrease of the lattice constants a, c , and the unit-cell volume V

TABLE I. The lattice constants a and c , the unit-cell volume V , and the intralayer nearest Mn–Mn distance $R_{\text{Mn–Mn}}^a$ for $\text{SmMn}_2(\text{Ge}_{1-x}\text{Si}_x)_2$ compounds.

x	a (Å)	c (Å)	V (Å ³)	$R_{\text{Mn–Mn}}^a$ (Å)
0.0	4.064	10.892	179.89	2.874
0.1	4.052	10.844	178.04	2.865
0.2	4.034	10.775	175.34	2.852
0.3	4.025	10.751	174.17	2.846
0.4	4.016	10.727	173.01	2.840
0.6	3.999	10.647	170.27	2.828
0.8	3.989	10.563	168.08	2.821
0.9	3.977	10.526	166.48	2.812
1.0	3.973	10.501	165.76	2.809

with increasing Si content x . This may be associated with the smaller atomic radius of Si compared with Ge. As a consequence of the decrease of the lattice parameters, the intralayer nearest Mn–Mn distance $R_{\text{Mn–Mn}}^a$ and the interlayer nearest Mn–Mn distance $R_{\text{Mn–Mn}}^c$ decrease as well. Figure 1 also shows $R_{\text{Mn–Mn}}^a$ as a function of the Si concentration and it can be seen that $R_{\text{Mn–Mn}}^a$ decreases linearly with increasing Si content. The values of the $R_{\text{Mn–Mn}}^a$ are also listed in Table I.

The temperature dependence of magnetization of the $\text{SmMn}_2(\text{Ge}_{1-x}\text{Si}_x)_2$ compounds measured in the temperature range 1.5–400 K in a field of 0.04 T is presented in Fig. 2. For the compounds with $x < 0.3$, three magnetic transitions are observed. The first transition occurs at the critical temperature T_1 , which strongly depends on the Si content and changes from about 40 to about 115 K. This is a transition from ferromagnetic (F) to antiferromagnetic (AF) order of the Mn moments. Below T_1 , the Sm sublattice is ferromagnetically ordered and is ferromagnetically coupled to the ferromagnetic Mn-sublattice moments due to the positive Sm–Mn exchange interaction.³ In the compounds with $x = 0.2$ and 0.3 , the magnetization increases with increasing temperature at the temperature lower than T_1 . This may be associated with the domain wall pinning occurring at low temperature in these samples. At T_1 already the magnetic ordering of the Sm sublattice collapses and Mn-sublattice magnetization is subject to a transition toward an antiferromagnetic configuration. With increasing temperature, at the second critical temperature T_2 , the transition from antiferromagnetism to ferromagnetism occurs. With further increasing temperature, at T_c , the transition from the ferromagnetic to the paramagnetic (P) phase is observed. Such a complex temperature-dependent magnetic behavior of the $\text{SmMn}_2(\text{Ge}_{1-x}\text{Si}_x)_2$ results from the strongly temperature-dependent nearest Mn–Mn distances and Sm–Mn exchange interaction. Since at room temperature the $R_{\text{Mn–Mn}}^a$ distance exceeds the critical value of about 2.85 Å, the Mn sublattice orders ferromagnetically. As temperature decreases the $R_{\text{Mn–Mn}}^a$ distance decreases, and it seems likely that, below T_2 , $R_{\text{Mn–Mn}}^a$ becomes smaller than the critical value of about 2.85 Å. Below T_1 the Sm sublattice magnetization becomes sufficiently strong to break the antiferromagnetic Mn–Mn coupling via the Sm–Mn coupling. For the compounds with $x > 0.3$, only one magnetic transition was observed, which corresponds to the transition at T_1 , from ferromagnetic to antiferromagnetic state (see Fig. 2).

Figure 3 shows the studied temperature dependence of susceptibility for the $\text{SmMn}_2(\text{Ge}_{1-x}\text{Si}_x)_2$ compounds with $x \geq 0.3$ in the temperature range from 300 to 1000 K in a magnetic field of 1.2 T by means of a Faraday balance. In the magnetic susceptibility curves $\chi(T)$ for compounds with $x \geq 0.3$, a maximum was observed, which corresponds to the transition from antiferromagnetic to paramagnetic state. The Néel temperature is defined by the cusp maximum of $\chi(T)$ and listed in Table II. The Néel temperature of SmMn_2Si_2 compound determined in this investigation is larger than that reported by Szytula and Szott.⁷ This may result from the fact that the magnetic field used in this investigation is higher than that used by Szytula and Szott.⁷

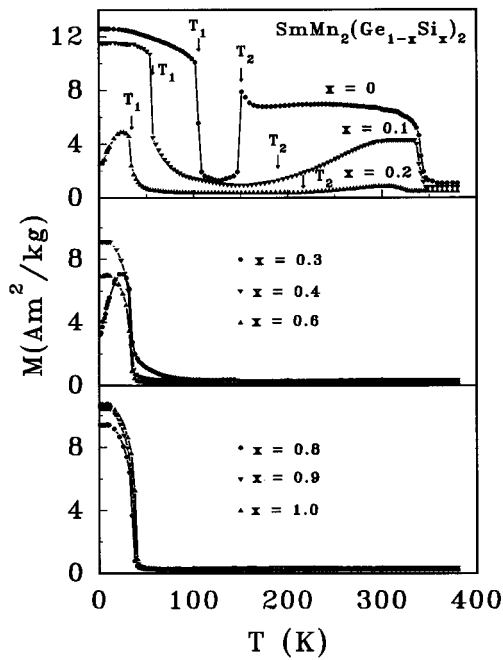


FIG. 2. Temperature dependence of the magnetization M in the temperature range 1.5–400 K for $\text{SmMn}_2(\text{Ge}_{1-x}\text{Si}_x)_2$ compounds in a magnetic field of 0.04 T.

Figure 4 shows the transition temperatures T_1 , T_2 , T_c , and T_N as functions of the Si content x and the inset in it shows those of $R_{\text{Mn-Mn}}^a$. The transition temperatures are also listed in Table II. The decrease of the Curie temperature with Si content may result from the decrease of magnetization of the Mn sublattice upon substitution of Si for Ge (see below). The second magnetic transition temperature T_2 increases from 140 K for $x=0$ –215 K for $x=0.2$ with increasing Si

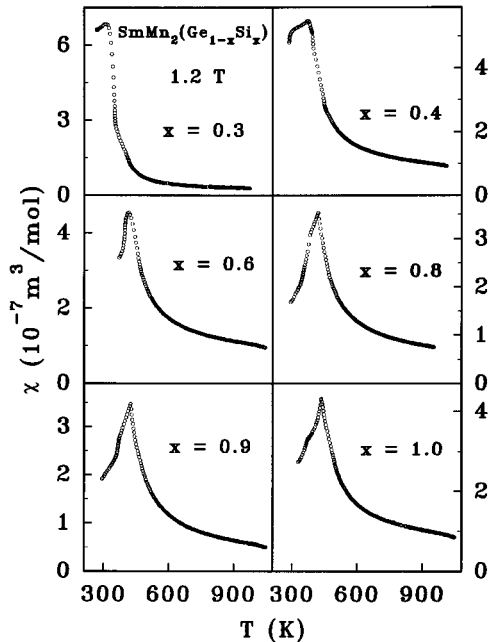


FIG. 3. Magnetic susceptibility χ vs temperature T of $\text{SmMn}_2(\text{Ge}_{1-x}\text{Si}_x)_2$ compounds measured at 1.2 T. The maximum of $\chi(T)$ defines T_N .

TABLE II. The ferromagnetic–antiferromagnetic transition temperature T_1 , the antiferromagnetic–ferromagnetic transition temperature T_2 , the Curie temperature T_c , the Néel temperature T_N , and the saturation magnetization M_s at 1.5 K and at room temperature for $\text{SmMn}_2(\text{Ge}_{1-x}\text{Si}_x)_2$ compounds.

x	T_1 (K)	T_2 (K)	T_c (K)	T_N (K)	M_s (1.5 K) ($\mu_B/\text{f.u.}$)	M_s (RT) ($\mu_B/\text{f.u.}$)
0.0	115	140	346		3.40	3.27
0.1	66	188	344		3.11	1.54
0.2	38	215	331		2.75	0.25
0.3	37			308	2.34	0.07
0.4	36			371	1.98	0.05
0.6	36			412	1.36	0.05
0.8	39			417	1.59	
0.9	40			420	1.68	
1.0	41			432	1.82	

content. This may originate from the decrease of $R_{\text{Mn-Mn}}^a$. Because the $R_{\text{Mn-Mn}}^a$ decreases with Si content, a higher temperature is needed to ensure that $R_{\text{Mn-Mn}}^a$ achieves or larger than 2.85 \AA . The value of T_1 first decreases, goes through a minimum at $x=0.4$ – 0.6 , and then increases slowly with increasing Si concentration. The decrease of T_1 with Si content x for a smaller x may result from the increase of the antiferromagnetic Mn–Mn coupling strength due to the decrease of the intralayer nearest Mn–Mn distance $R_{\text{Mn-Mn}}^a$ upon substitution of Si for Ge, whereas the slight increase of T_1 with Si content for $x>0.6$ may result from the decrease of the Mn-sublattice moments due to the substitution of Si for Ge, which leads to a slight decrease in the Mn–Mn antiferromagnetic exchange interaction in the Mn sublattice. The Néel temperature T_N increases monotonically with increasing Si concentration. This also results from the enhancement of the negative Mn–Mn exchange interaction on Si substitution for

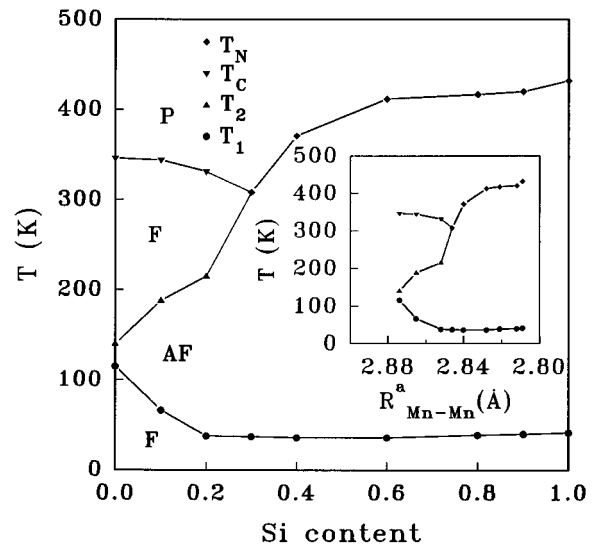


FIG. 4. Phase diagram of $\text{SmMn}_2(\text{Ge}_{1-x}\text{Si}_x)_2$. The ferromagnetic–antiferromagnetic transition temperature T_1 , the antiferromagnetic–ferromagnetic transition temperature T_2 , the Curie temperature T_c , and the Néel temperature T_N for $\text{SmMn}_2(\text{Ge}_{1-x}\text{Si}_x)_2$ compounds obtained in this investigation can be identified. Inset: T_1 , T_2 , T_c , and T_N as function of the intralayer nearest Mn–Mn distance $R_{\text{Mn-Mn}}^a$ for the $\text{SmMn}_2(\text{Ge}_{1-x}\text{Si}_x)_2$ compounds.

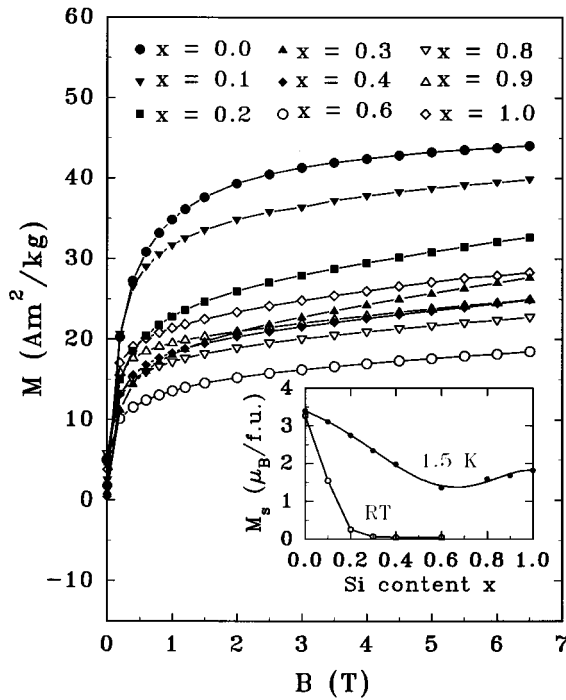


FIG. 5. Magnetization curves at 1.5 K for the $\text{SmMn}_2(\text{Ge}_{1-x}\text{Si}_x)_2$ compounds. Inset: The saturation magnetization at 1.5 K and at room temperature as a function of Si concentration x for the $\text{SmMn}_2(\text{Ge}_{1-x}\text{Si}_x)_2$ compounds.

the decrease of the intralayer nearest Mn–Mn distance $R_{\text{Mn-Mn}}^a$. Figure 4 is a spin phase diagram for $\text{SmMn}_2(\text{Ge}_{1-x}\text{Si}_x)_2$, which divided the temperature–Si-content plane by several areas which correspond to the different magnetic order, as pointed out in Fig. 4. The magnetic phase diagram we obtained is very similar to that of the $\text{Sm}_{1-x}\text{Gd}_x\text{Mn}_2\text{Ge}_2$ system⁹ and that of the $\text{Sm}_{1-x}\text{Y}_x\text{Mn}_2\text{Ge}_2$ system.¹⁰

The magnetization of the $\text{SmMn}_2(\text{Ge}_{1-x}\text{Si}_x)_2$ compounds as a function of applied magnetic field was measured at 1.5 K in applied fields up to about 7 T (Fig. 5). The values of the saturation magnetization at 1.5 K as a function of Si content are shown as an inset in Fig. 5 and also listed in Table II. It can be seen that the saturation magnetization first decreases, goes through a minimum at about $x=0.6$, and then increases again with increasing Si concentration. Neglecting the contribution of the Sm atoms to the magnetic moments, the Mn atomic moment in $\text{Sm}_2\text{Mn}_2\text{Ge}_2$ was derived to be $1.7\mu_B$. This value is too small compared with $3\mu_B$, which corresponds to three unpaired electrons in the $3d$ shell. Szytula and Siek⁴ have explained the small Mn moment in the ThCr_2Si_2 type of crystal structure by means of the spin transfer from the $3p$ shell of Si to the $3d$ shell of Mn. Since substitution of Si for Ge give rise to a decrease of the lattice constants a , which leads to a increasing overlap of the $3p$ state of Si or Ge with the $3d$ state of Mn, and more and more spin transfer from the $3p$ shell to the $3d$ shell of Mn, resulting in a further decrease of magnetic moment on the Mn atoms with increasing Si content. The increase of the saturation magnetization of the $\text{SmMn}_2(\text{Ge}_{1-x}\text{Si}_x)_2$ compounds with Si content $x>0.6$ may associate with the increase of the

ferromagnetic coupling between Sm and Mn moments due to the decrease of the interlayer nearest Mn–Mn distance $R_{\text{Mn-Mn}}^c$ with Si content x increasing, which leads to more Mn moments aligning along the c axis.

The magnetization curves at room temperature have been measured by using pulsed magnetic fields up to 10 T. The values for the saturation magnetization as a function of Si content are also shown in the inset in Fig. 5 and it can be seen that the saturation magnetization decreases monotonically with the Si content. This is due to a gradual transition of the magnetic order of the Mn moments on the Mn sublattice from ferromagnetic for $x=0$ to antiferromagnetic for $x=0.3$.

CONCLUSION

In conclusion, all $\text{SmMn}_2(\text{Ge}_{1-x}\text{Si}_x)_2$ compounds with $x=0-1.0$ crystallize in ThCr_2Si_2 type of structure. Substitution of Si for Ge leads to a linear decrease in the lattice constants a , c , and the unit-cell volume V from $a=4.064 \text{ \AA}$, $c=10.892 \text{ \AA}$, $V=179.89 \text{ \AA}^3$ for $x=0$ to $a=3.973 \text{ \AA}$, $c=10.501 \text{ \AA}$, $V=165.76 \text{ \AA}^3$ for $x=1.0$. The intralayer nearest Mn–Mn distance $R_{\text{Mn-Mn}}^a$ decreases linearly from 2.874 \AA for $x=0$ to 2.809 \AA for $x=1.0$. In all compounds a magnetic transition from ferromagnetic to antiferromagnetic is observed at lower temperatures T_1 , which decreases first, goes through a minimum at $x=0.4-0.6$, and then increases slightly with Si content. With increasing temperature, for the compounds with $x<0.3$ both antiferromagnetic–ferromagnetic transition and ferromagnetic–paramagnetic transition are observed as well at T_2 and T_c , respectively. The former increases and but the latter decreases with Si content. For compounds with $x\geq 0.3$ the antiferromagnetic–paramagnetic transition is observed and the Néel temperature increases monotonically with Si content. A tendentious spin phase diagram has been obtained. Substitution of Si for Ge leads to an increase of the antiferromagnetic–ferromagnetic transition temperature T_2 from 140 K at $x=0$ to 215 K at $x=0.2$. The increase of T_2 is important for practical application of the magnetoresistance effect. The saturation magnetization at 1.5 K decreases first, goes through a minimum at $x=0.6$, and then increases again. The saturation magnetization at room temperature decreases monotonically from $3.27\mu_B/\text{f.u.}$ for $x=0$ to nearly zero for $x=0.3$. These changes in the magnetic properties can be quite well understood by means of the variation in the intralayer and interlayer nearest Mn–Mn distances and Sm–Mn exchange interaction with Si concentration.

ACKNOWLEDGMENT

The present investigation has been carried out within the scientific exchange program between China and The Netherlands, and was supported by the National Natural Science Foundation of China.

¹Z. Ban and M. Sikirica, *Acta Crystallogr.* **18**, 594 (1965).

²A. Szytula and J. Leciejewicz, in *Handbook of Physics and Chemistry of Rare Earths*, edited by K. A. Gschneidner, Jr. and L. Eyring (North-Holland, Amsterdam, 1989), Vol. 12, p. 133.

³H. Fujii, T. Okamoto, T. Shigeoka, and N. Iwata, *Solid State Commun.*

53, 715 (1985); *J. Magn. Magn. Mater.* **54–57**, 1345 (1986).

⁴A. Szytula and S. Siek, *J. Magn. Magn. Mater.* **27**, 49 (1982).

⁵J. H. V. J. Brabers, A. J. Noltén, F. Kayzel, S. H. J. Lenczowski, K. H. J. Buschow, and F. R. de Boer, *Phys. Rev. B* **50**, 16 410 (1994).

⁶M. Duraj, R. Duraj, A. Szytula, and Z. Tomkowicz, *J. Magn. Magn. Mater.* **73**, 240 (1988).

⁷A. Szytula and I. Szott, *Solid State Commun.* **40**, 199 (1981).

⁸J. H. V. J. Brabers, K. Bakker, H. Nakotte, F. R. de Boer, S. K. J. Lenczowski, and K. H. J. Buschow, *J. Alloys Compd.* **199**, L1 (1993).

⁹M. Duraj, R. Duraj, and A. Szytula, *J. Magn. Magn. Mater.* **79**, 61 (1989).

¹⁰M. Duraj, R. Duraj, and A. Szytula, *J. Magn. Magn. Mater.* **82**, 319 (1989).